Journal of Sound and Vibration (2002) **253**(4), 795–805
doi:10.1006/jsvi.2001.3805, available online at http://www.idealibrary.com on IDEAL®

AERODYNAMIC DAMPING OF RANDOMLY EXCITED PLATES IN STATIONARY AND MOVING AIR

A. Z. TARNOPOLSKY, J. C. S. LAI AND N. H. FLETCHER†

School of Aerospace and Mechanical Engineering, University College, The University of New South Wales, Australian Defence Force Academy, Canberra 2600, *Australia.*
E-mail: *j.lai@adfa.edu.au*

(*Received* 13 *October* 2000, *and in final form* 3 *April* 2001)

An experimental study of the aerodynamic damping of oscillating plates has been undertaken. Plates of various shapes were placed into an air flow normal to the plate and excited to oscillate parallel to the flow direction by electromagnetic forces of equal amplitudes and random frequencies. The aerodynamic damping of oscillating plates, evaluated in terms of a quality Q-factor from a frequency response resonance curve, was found to vary linearly with the absolute pressure in stationary surrounding air and with the air flow velocity in moving air. The flow velocity was also found to affect the aerodynamic damping more than the absolute pressure. A simple empirical model has been developed to predict the variation of the aerodynamic damping with the flow velocity.

1. INTRODUCTION

There have been extensive studies of the behaviour of pressure-controlled self-oscillating valves in woodwind instruments [1–5]. Despite the geometric and dynamic complexities of various valves, the mechanism of self-oscillation was found to be commonly based on oscillating pressure forces induced by the valve motion [6].

It has proved helpful to classify the valves according to the effect of the upstream or downstream overpressure on the tendency of the valves to open further or to close. Thus, the valve will be called blown-closed when upstream overpressure tends to close the valve and downstream overpressure tends to open it. Similarly, the valve will be called blown-open when the upstream blowing pressure tends to open the valve (see Figure 1). Woodwind-type reeds are good examples of blown-closed valves while the human larynx and players lips in brass musical instruments could be considered as blown-open valves. A detailed explanation of the valve classification with a description of different types of pressure-controlled valves may be found in Fletcher [6].

The mechanism of self-oscillations of blown-open valves was studied experimentally recently [6, 7]. Even when the velocity of the jet through the valve is very small, jet separations on the valve edges cause the development of a random turbulence of broad frequency spectrum. The turbulence gives rise to unsteady pressure forces which excite random vibration of the valves of small amplitude of the order of the valve thickness. The small vibration is unstable and, when the pressure forces overcome damping, the valve

† Permanent address. Research School of Physical Sciences and Engineering, Australian National University, Canberra 0200, Australia.

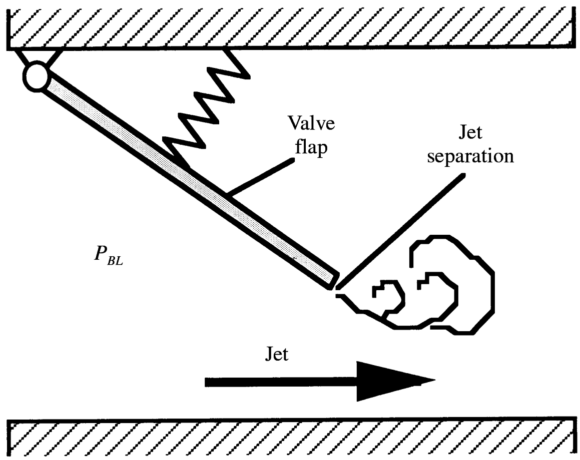

Figure 1. Schematic of blown-open pressure-controlled self-oscillating valves, where P_{BL} is the upstream blowing pressure.

vibration tends to grow rapidly to large amplitude establishing self-oscillations with the frequency close to the valve resonance frequency. The amplitude of large oscillations was found to be of the order of the jet thickness. A quasi-steady approximation to time-varying flow gives a good estimate of the threshold pressure [6] of self-oscillations.

The theoretical and experimental studies [6, 7] suggest that the valve oscillations largely depend on the damping characteristics of the valve. Since damping is contributed both by internal material losses and by aerodynamic effects, knowledge about the aerodynamic damping is important.

The aerodynamic damping has received much attention in the past. Beginning with Stokes' classical paper on the motion of pendulums in unlimited viscous fluid [8], most of the work is, however, related to a body oscillating in a stationary surrounding with a relatively small Reynolds number. The aerodynamic damping in these cases is mostly due to large viscous forces [9–11]. Studies of body oscillation in a cross flow shows a large dependency of the aerodynamic damping on the vortex development [12]. Recent flow visualization results of a pressure-controlled self-oscillating valve also show the development of a stable vortex downstream of the valve [13]. However, it was found that the vortex does not affect much the valve self-oscillation [4, 13].

The aerodynamic damping of a pressure-controlled self-oscillating valve of musical instruments has not received much attention in the past. In order to simplify the analysis, we examine the aerodynamic damping of an oscillating plate placed into an air flow perpendicular to the plane of the plate and oscillated parallel to the flow direction.

2. BACKGROUND THEORY

Since the ratio of the dissipated energy E_D to the mechanical energy E_M of an oscillating system is inversely proportional to a so-called quality factor Q, it is a common practice to represent the damping of an oscillating system by using the Q-factor [14]:

$$\frac{E_D}{E_M} = \frac{2\pi}{Q}. \tag{1}$$

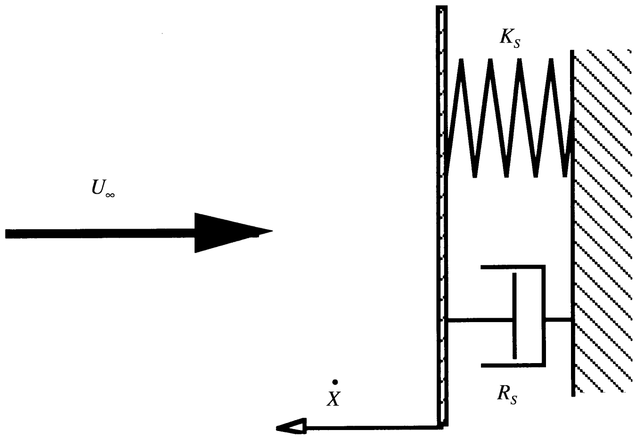

Figure 2. Schematic of the theoretical model of the plate oscillation in air flow.

Our aim of the following theoretical development is to establish a relationship between the aerodynamic damping in terms of the quality Q-factor and parameters of a self-oscillating valve.

In the following analysis, the pressure-controlled self-oscillating valve is simplified to a plain rectangular plate placed into a potential air flow perpendicular to the plane of the plate and harmonically oscillated parallel to the flow direction (see Figure 2). Since all forces acting on the plate must be in balance, the equation of motion of the oscillating plate can be written as

$$m_S\ddot{x} + R_S\dot{x} + K_S x = F_A, \tag{2}$$

where m_S is the mass of the plate, R_S is the structural damping coefficient, K_S is the structural stiffness and F_A is the aerodynamic force [6]. Here, subscripts S and A refer to internal structural forces and external aerodynamic forces respectively.

Assuming that the motion of the plate is much smaller than its size, the first order expansion of the aerodynamic force may then be written in the form [15]

$$F_A(x, \dot{x}) = F_{A0} + \frac{\partial F_A}{\partial x}(x - x_0) + \frac{\partial F_A}{\partial \dot{x}}(\dot{x} - \dot{x}_0), \tag{3}$$

where x is the co-ordinate of the plate in the flow direction, x_0 is the equilibrium position of the plate where the velocity is $\dot{x}_0$, and F_{A0} is the aerodynamic force at the equilibrium position. Note that F_{A0} is the constant of the aerodynamic force and may be interpreted as the drag force of a stationary plate in a steady flow. For analysis it is more convenient to select the equilibrium position such that $\dot{x}_0 = 0$ which is associated with a steady motion. Assuming that the plate oscillates harmonically with $x = A_x\cos(\omega t)$, the equilibrium position is then $x_0 = A_x$, $\dot{x}_0 = 0$. Substituting equation (3) into equation (2), we have

$$m_S\ddot{x} + R_\Sigma\dot{x} + K_\Sigma(x - A_x) = F_{A0}. \tag{4}$$

Here the second term represents a damping force due to the combined effect of structural and aerodynamic energy dissipations with $R_\Sigma = R_S - \partial F_A/\partial\dot{x}$. The third term is the flexible force due to the combined effect of structural and aerodynamic stiffness of the oscillating system [15], with $K_\Sigma = K_S - \partial F_A/\partial x$. Since F_{A0} is associated with a steady motion, it is related to the drag coefficient C_D as

$$F_{A0} = \tfrac{1}{2}\, C_D \rho S U_\infty^2, \tag{5}$$

where ρ is the density of the fluid, U_∞ is the fluid velocity and S is the surface area of the plate. It can be seen from equation (4) that since F_{A0} is the constant part of the aerodynamic force, it does not have any effect on the aerodynamic damping.

The damping energy is then

$$E_D = \int_0^T \left(R_S - \frac{\partial F_A}{\partial \dot{x}} \right) \dot{x}^2 \, \mathrm{d}t. \tag{6}$$

Aerodynamic force, on the other hand, is due to momentum exchange between a flow stream and a moving object and is proportional to the product of the mass flow and the velocity of the object in relative motion:

$$F_A = \frac{C_p}{2} \rho S (U_\infty - \dot{x}) | U_\infty - \dot{x} |, \tag{7}$$

where C_p is the coefficient of proportionality. For steady flows, this coefficient is equal to the drag coefficient and is well defined experimentally for many different body shapes [16]. The coefficients differ for unsteady cases [9], however, and have therefore to be defined for the present case.

It is reasonable to assume that in musical instruments the flow velocity is larger than the velocity of the valve oscillation and therefore we always would have $(U_\infty - \dot{x}) > 0$. The force derivatives with respect to the plate velocity can then be obtained from equation (7) as

$$\frac{\partial F_A}{\partial \dot{x}} = -\, C_p \rho S (U_\infty - \dot{x}). \tag{8}$$

Substituting equation (8) into equation (6) and using $x = A_x \cos(\omega t)$, the integral in equation (6) can be then expressed in the form

$$E_D = \pi \omega A_x^2 \left[R_S + C_p \left(\rho S U_\infty + \frac{8}{3\pi} \omega \rho S A_x \right) \right]. \tag{9}$$

The mechanical energy of the oscillating system can be defined as

$$E_M = E_K + E_P = (E_K)_{MAX} = (E_P)_{MAX} = \tfrac{1}{4}\, m_S \omega^2 A_x^2, \tag{10}$$

where E_K is the kinetic energy, E_P is the potential energy and subscript MAX refers to maximum. Finally, the ratio of the dissipated energy to the mechanical energy during one period of the valve oscillation can be obtained from equations (9) and (10) as

$$\frac{2\pi}{Q} = \frac{E_D}{E_M} = \frac{4\pi}{m_S \omega} R_S + \frac{4\pi}{m_S \omega} R_A. \tag{11}$$

Here we introduce a resistance constant R_A due to the aerodynamic damping

$$R_A = C_p \left(\rho S U_\infty + \frac{8}{3\pi} \omega \rho S A_x \right). \tag{12}$$

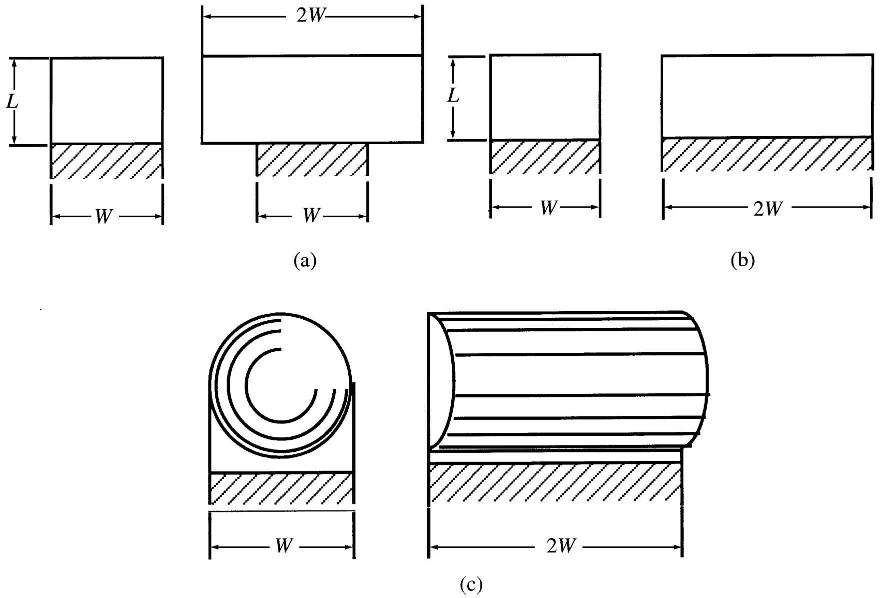

Figure 3. Plates of various sizes and shapes used to measure aerodynamic damping; (a) in stationary surrounding; (b) and (c) in the wind tunnel.

Note that $\rho S U_\infty$ in equation (12) is the mass flow on the valve cross-section due to the plate steady motion and $\omega \rho S A_x / \pi = 2\rho S A_x / T$ is the mass of displaced air during one period of the plate oscillation and $T = 2\pi/\omega$ is the period of the plate oscillation. Thus, the aerodynamic damping arises from the energy dissipation due to the steady plate motion and the oscillating plate motion. According to equation (12), the first term of the aerodynamic damping varies linearly with the flow velocity and the second term varies linearly with the amplitude and the frequency of the plate oscillation. Furthermore, the second term in equation (12) represents the aerodynamic damping of a plate oscillating in stationary air and is a constant for a given plate at a given absolute pressure. Thus from equation (12), the aerodynamic damping of a plate oscillating in moving air varies linearly with the free stream velocity U_∞ at a given absolute pressure. In order to evaluate the structural and aerodynamic damping and to verify these theoretical results, the experiments described below were conducted.

3. EXPERIMENT

Plates of various sizes and shapes were placed in a steady air flow normal to the plate and were excited to oscillate parallel to the flow. Figure 3 shows the configurations of the various plates tested. The plate flaps were cut from a flat brass sheet of 0·15 mm thickness.

In order to obtain the frequency response resonance curve, an exciting force of constant amplitude and random frequency was applied to the plate using an electromagnet. A small permanent magnet of mass 184 g was glued to the valve surface. The valve response was measured using a small B&K type 4734 accelerometer with a dynamic mass of 0·65 g. The accelerometer was placed close to the clamping end of the valve to minimize the effect on the valve behaviour.

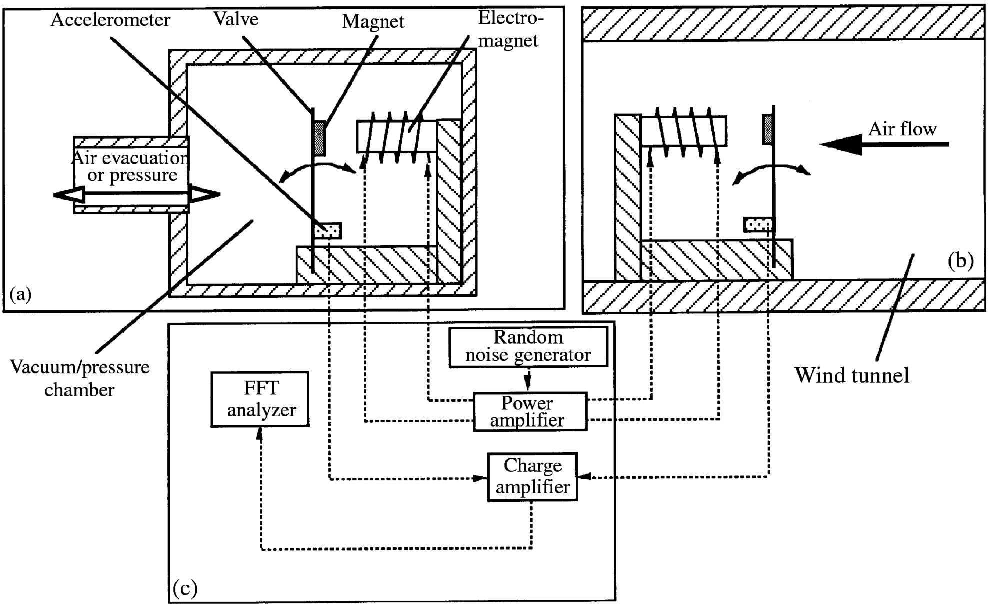

Figure 4. Schematic of the experimental set-up: (a) measurements in stationary air using vacuum/pressure chamber; (b) measurements in the wind tunnel: (c) instrumentation.

Figure 4 shows the schematic of the instrumentation set-up including a small B&K 4734 accelerometer, an ONOSOKI dual channel FFT analyser, B&K power (Type 2706) and charge (Type 2635) amplifiers and a random noise generator covering a frequency band from 0 to 200 Hz with a frequency resolution of 0·125 Hz.

First, the aerodynamic damping was measured in a stationary surrounding air. Thus, two plain plates of thickness 0·15 mm and dimensions 35 mm × 30 mm and 70 mm × 30 mm (see Figure 3(a)) were each placed into a specially made vacuum/pressure chamber and the frequency response resonance curves were obtained at various absolute pressures from 1 to 800 kPa. In order to reduce the effect of the structural damping, the clamping length of the second plate was made 35 mm similar to the first plate (see Figure 3(a)).

After completing the measurements in the vacuum/pressure chamber, the set-up with the plates was placed into a wind tunnel with the flow normal to the plate. The frequency response resonance curves were then obtained for various flow velocities. Two valves of different frontal shapes were also tested: a hemisphere of diameter 35 mm and a semicylinder of diameter 35 mm and length 70 mm (see Figure 3(c)).

The procedure used to evaluate the aerodynamic damping in terms of the Q-factor from the experimentally determined frequency response resonance curves is described in the appendix.

4. EXPERIMENTAL RESULTS AND DISCUSSIONS

Since the frequency response data were obtained over 1000 cycles of oscillation, the Q-factor was determined as an average rather than an instantaneous value. Figure 5 shows some typical experimental frequency response resonance curves measured by the accelerometer for the randomly excited rectangular plates in stationary surrounding air

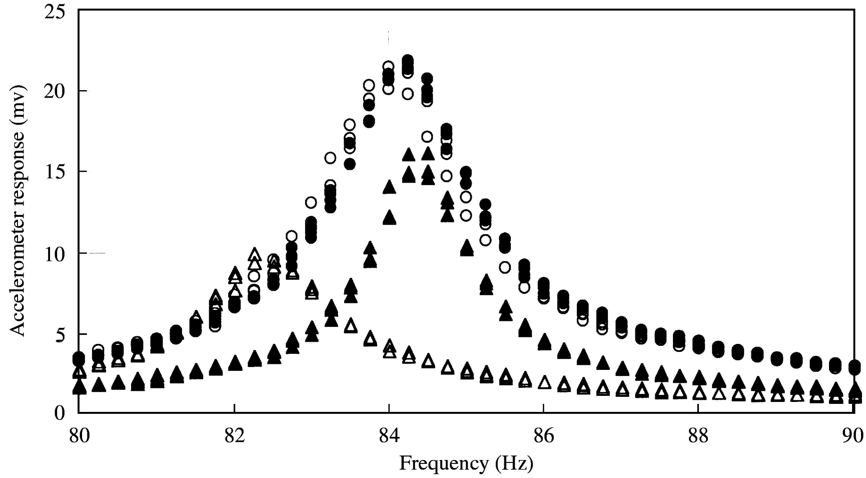

Figure 5. Experimental frequency response resonance curves of plates of various sizes oscillating in stationary surrounding air for various absolute pressure. ● Plate, 35 mm × 30 mm; $P = 1$ kPa; ○ Plate, 35 mm × 30 mm; $P = 800$ kPa; ▲ Plate, 70 mm × 30 mm; $P = 1$ kPa; △ Plate, 70 mm × 30 mm; $P = 800$ kPa.

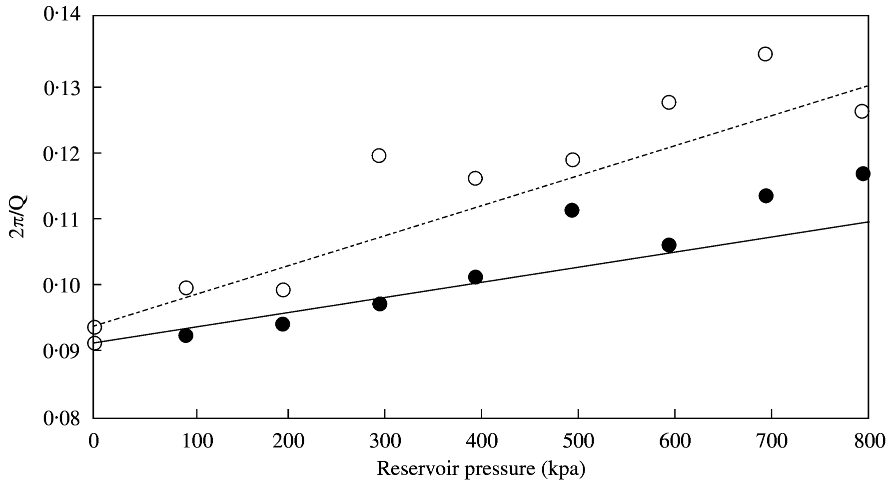

Figure 6. Variation of aerodynamic damping of oscillating plates in stationary air with absolute pressure. ●, experiments with plate 35 mm × 30 mm; ○, experiments with plate 70 mm × 30 mm; ——, equation (11) (plate 35 mm × 30 mm); -------, equation (11) (plate 70 mm × 30 mm).

using the vaccum/pressure chamber. It is obvious that the Q-factor incorporates both structural and aerodynamic damping.

Figure 6 shows the variation with absolute pressure of the damping $2\pi/Q$ of a plate oscillating in stationary air. It can be seen that $2\pi/Q$ varies linearly with the absolute pressure. Since the temperature of air was kept constant, this linear variation with pressure can also be interpreted as a linear variation with density. A linear function was then fitted to the experimental data using the least-squares method. The fitted function at zero pressure gives an estimate of the average structural damping in terms of the Q-factor. Theoretically, the structural damping should be the same for both valve configurations because the size of

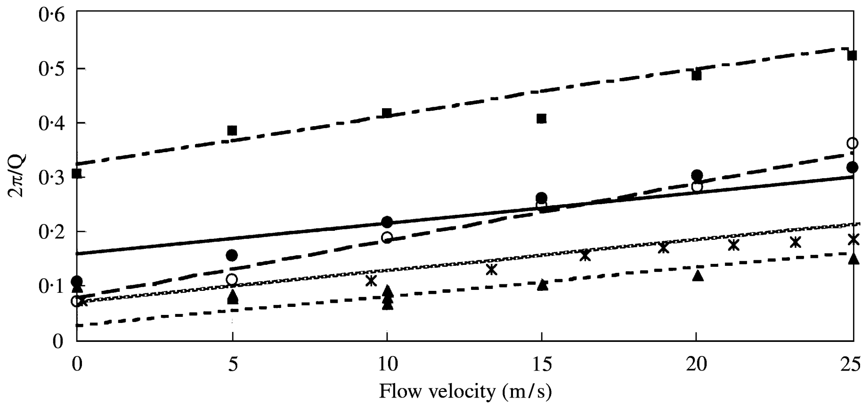

Figure 7. Variation of aerodynamic damping of oscillating plates in wind tunnel with flow velocity. ●, experiments with plate 35 mm × 36 mm; ——, equation (11) (plate 35 mm × 36 mm); ○, experiments with plate 70 mm × 36 mm; -------, equation (11) (plate 70 mm × 36 mm); ▲, experiments with semi-cylinder $D = 35$ mm; ▬ ▬ ▬, equation (11) (semi-cylinder $D = 35$ mm); ■, experiments with hemisphere $D = 38$ mm; ▬ ▪ ▪, equation (11) (hemisphere $D = 38$ mm); ✖, experiments with plate attached to reservoir; ▭▭▭, equation (11) (plate attached to reservoir).

clamping edges in both cases was kept the same. In practice, it was not easy to ensure the same clamping conditions during the change from one plate to another because of various factors such as clamping screw tension, accelerometer placement. It can be seen from Figure 6 that at normal atmospheric pressure, the damping increase due to the aerodynamic damping is small compared to the structural damping.

In order to calculate the aerodynamic damping in stationary air, the flow velocity in equation (12) was set equal to zero and the coefficient of proportionality C_P was taken as unity. The experimental coefficient R_S of the average structural damping at zero absolute pressure was used for the calculations. Figure 6 shows that equation (11) predicts sufficiently well the variation of the aerodynamic damping with the absolute pressure. According to equation (11), if we increase the area of the plate, the ratio $2\pi/Q$ would not increase because the mass of the plate would also increase by the same amount. However, the mass m_S in equation (11) is the mass moved by the exciting force. In our case this is the effective mass which consists of the mass of the constant magnet and the plate. The magnet has nearly the same mass as the plate and is glued at about $\frac{1}{3}$ length from the moving edge of the plate. Therefore, when the plate area is doubled, the effective mass is increased by only 1·34 times and, as a result, we have an increase of $2\pi/Q$ by about 1·5 times.

Measurements of the aerodynamic damping were then performed in a wind tunnel with the flow direction being normal to the plane of the plates. Two flat plates similar to the previous experiment (see Figure 3(b)) were tested first. The experimental results in Figure 7 show that the aerodynamic damping varies linearly with the flow velocity. The different slopes of the graphs can still be explained by the fact that the increase in the effective mass is less than the increase in the area when the plate area is doubled.

In order to evaluate the effect of the constant part of the aerodynamic forces on the aerodynamic damping (see equation (5)), two other valves, one with an upstream hemispherical cross-section of 35mm diameter, and another valve of dimensions 70 mm × 36 mm with a semicylinder 35 mm in diameter and with the plate clamping length of 70 mm (see Figure 3(c)) were tested. According to reference [16], when a hemisphere is placed on a plate, the drag coefficient in equation (5) is reduced from about 1·9 to about 0·42 and when a semicylinder is placed on a plate, the drag coefficient is reduced to about 1·15.

The constant part of the aerodynamic force (see equation (5)) was therefore reduced relative to the flat plate by a factor of 4·5 for the hemisphere and by a factor of 1·6 for the semicylinder.

The results of the measurements are shown in Figure 7. It can be seen that the plate with semicylinder shows a minimum damping for a flow velocity of about 10 m/s, but above this velocity, damping increases linearly with the flow velocity. It is interesting to note that irrespective of plate shapes and sizes, the damping increases linearly with the flow velocity. According to equation (5), the constant part of the aerodynamic forces acting on an oscillating plate is associated with the drag in steady flow and therefore has no effect on the aerodynamic damping of oscillating plates in moving air. The simple model as given by equations (11) and (12) indicates that the aerodynamic damping of plates oscillating in moving air varies linearly with the flow velocity at a given absolute pressure. It can be seen from Figure 7 that equation (11) gives a reasonably good prediction of the aerodynamic damping with $C_P = 1$ for all cases regardless of plate shapes and sizes.

The flow was not constrained in the wind tunnel experiments and was free to move around the plates. In pressure-controlled self-oscillating valves attached to a pressure reservoir over an aperture of size similar to the plate [7], the flow becomes constrained, escaping from the reservoir as a jet through a small gap between the valve and the reservoir wall in a direction nearly parallel to the plane of the valve. Another experiment was therefore performed in order to measure the aerodynamic damping in constrained air flow. Thus, a plate of thickness 0·15 mm and dimensions 52 mm $\times$ 30 mm was placed on a large reservoir over an aperture of size just equal to that of the plate. The volume of the reservoir was large enough to avoid plate self-oscillations [7]. Then the variation of quality Q-factor with jet velocity was examined, the jet velocity being calculated from the reservoir blowing pressure. The result of the measurements is also presented in Figure 7.

It can be seen in Figure 7 that the variation of Q-factor with flow velocity is very similar between constrained and non-constrained flow. The results indicate that the aerodynamic damping varies linearly with the flow velocity and does not depend significantly on the flow direction. It is interesting to note that equation (11) gives a reasonably good prediction of the aerodynamic damping when the coefficient of proportionality in the equation is taken as $C_P = 1$, as in all other cases.

Comparison between the experimental results in Figures 6 and 7 reveals that within the range of pressure and velocity tested, the aerodynamic damping depends more on the flow velocity than on the absolute pressure. For example, a five times increase in flow velocity would nearly double the aerodynamic damping whereas an increase of the absolute pressure from 1 to 800 kPa gives only about 20% increase in the aerodynamic damping.

5. CONCLUSIONS

The aerodynamic damping of oscillating plates of various shapes and sizes has been studied experimentally in stationary and moving air. The experimental results show that the aerodynamic damping of plates oscillating in stationary air varies linearly with absolute pressure. The aerodynamic damping of a rectangular plate oscillating in stationary air at atmospheric pressure is small compared with structural damping for the plates tested. The measurements in a wind tunnel show that the aerodynamic damping of oscillating plates at atmospheric pressure is much larger in moving air than in stationary air. Furthermore, the aerodynamic damping of oscillating plates in moving air at atmospheric pressure varies linearly with the flow velocity. The measurements show insignificant difference between the aerodynamic damping obtained when the air flow is constrained and that when it is not constrained.

A simple model has been developed to predict the aerodynamic damping of oscillating plates in stationary and moving air. The simple model suggests that the constant part of aerodynamic forces is associated with the drag of a stationary plate in steady flow and therefore does not have any effect on the aerodynamic damping of oscillating plates. It was found that for oscillating plates, the coefficient of proportionality of $C_P = 1$ gives a reasonably good prediction for all the experimental cases irrespective of the plate sizes and shapes. Thus, unlike the drag coefficient for a stationary plate in steady flow, the coefficient of proportionality C_P for oscillating plates appears to be independent of the plate shapes and Reynolds number for the conditions tested.

ACKNOWLEDGMENTS

This study forms part of a project supported by a grant from the Australian Research Council.

REFERENCES

1. N. H. Fletcher 1979 *Acustica* **43**, 63–72; erratum in **50**, 155–159 (1982). Excitation mechanisms in woodwind and brass instruments.
2. S. J. Elliot and J. M. Bowsher 1982 *Journal of Sound and Vibration* **83**, 181–217. Regeneration in brass wind instruments.
3. D. C. Copley and W. J. Strong 1996 *Journal of Acoustic Society of America* **99**, 1219–1226. A stoboscopic study of lip vibrations in a trombone.
4. A. O. St Hilaire, T. A. Wilson and G. S. Beavers 1971 *Journal of Fluid Mechanics Part* 4 **49**, 803–816. Aerodynamic excitation of the harmonium reed.
5. N. H. Fletcher and T. D. Rossing 1998 *The Physics of Musical Instruments*, New York: Springer-Verlag; second edition.
6. N. H. Fletcher 1993 *Journal of Acoustic Society of America Part* 1 **93**, 2172–2280. Autonomous vibration of simple pressure-controlled valves in gas flows.
7. A. Z. Tarnopolsky, N. H. Fletcher and J. C. S. Lai 2000 *Journal of Acoustic Society of America* **108**, 400–406. Oscillating reed valves—an experimental study.
8. G. G. Stokes 1851 *Transactions of the Cambridge Philosophical Society* **9**, 8. On the effect of the internal friction of fluids on the motion of pendulums.
9. G. H. Keulegan and L. H. Carpenter 1958 *Journal of Research of the National Bureau of Standards* **60**, 423–440. Forces on cylinders and plates in an oscillating fluid.
10. P. W. Bearman, M. J. Downie, J. M. R. Graham and E. D. Obasaju 1985 *Journal of Fluid Mechanics* **154**, 337–356. Forces on cylinders in viscous oscillatory flow at low Keulegan–Carpenter numbers.
11. P. Anagnostopoulos and G. Iliadis 1998 *Journal of Fluids and Structures* **12**, 225–258. Numerical study of the flow pattern and the in-line response of a flexible cylinder in an oscillating stream.
12. C. Y. Zhou, R. M. C. So and K. Lam 1999 *Journal of Fluids and Structures* **13**, 165–189. Vortex-induced vibrations of an elastic circular cylinder.
13. A. Z. Tarnopolsky, J. C. S. Lai and N. H. Fletcher 2001 *Journal of Sound and Vibration* **247**(2), 213–226. Flow structures behind pressure-controlled self-oscillating reed valves (submitted).
14. L. E. Kinsler, A. R. Frey, A. B. Coppens and J. V. Sanders 1982 *Fundamentals of Acoustics*. New York: John Wiley & Sons.
15. P. Hemon 1999 *Journal of Fluids and Structures* **13**, 291–307. An improvement of the time delayed quasi-steady model for the oscillations of circular cylinders in cross-flow.
16. B. R. Munson, D. F. Young and T. H. Okiishi 1998 *Fundamentals of Fluid Mechanics*. New York: John Wiley & Sons Inc.
17. D. J. Ewins 1984 *Modal Testing: Theory and Practice*. New York: Research Studies Press Ltd., John Wiley & Sons.

APPENDIX A: DETERMINATION OF Q-FACTOR FROM FREQUENCY RESPONSE CURVES

The frequency response of an oscillating system with a single degree of freedom is given by [17]

$$\alpha(\omega) = \frac{1}{\sqrt{(K_\Sigma - \omega^2 m)^2 + (\omega_0 R_\Sigma)^2}}, \tag{A.1}$$

where $\alpha(\omega)$ is the magnitude of receptance. However, because the experimental frequency response data of the oscillating plate was obtained by using an accelerometer, the inertance of the oscillating system rather than the receptance was acquired. Therefore, since $\omega_0^2 = K_\Sigma / m_S$ and $Q = \omega_0 m_S / R_\Sigma$, the experimental frequency response data from the accelerometer can be described by

$$V = \frac{A\omega^2}{m_S \sqrt{(\omega_0^2 - \omega^2)^2 + (\omega_0 \omega / Q)^2}}, \tag{A.2}$$

where V denotes the signal value measured by the accelerometer in millivolts and A is a scale coefficient. In order to evaluate the Q-factor from the experimental data, equation (A.2) can be written as a second order equation

$$y = a_1 x^2 + a_2 x + a_3, \tag{A.3}$$

where $y = (1/V)^2$, $x = (1/\omega)^2$ and the coefficients a_1, a_2, and a_3 are

$$a_1 = \omega_0^4 \left(\frac{m_S}{A}\right)^2, \quad a_2 = \omega_0^2 \left(\frac{m_S}{A}\right)^2 \left(\frac{1}{Q^2} - 2\right), \quad a_3 = \left(\frac{m_S}{A}\right)^2. \tag{A.4}$$

By fitting a second order polynomial to the experimental data near the peak of the response curve using the least-squares method, the values of the coefficients a_1, a_2 and a_3, in equations (A.4) were obtained. The three equations in (A.4) were then solved to give an estimate of the Q-factor.